Support information

Model-Based Analysis for Ethylene Carbonate Hydrogenation Operation in Industrial-Type Tubular Reactors

Hai Huang [1], Chenxi Cao [2,*], Yue Wang [3], Youwei Yang [3], Jianning Lv [4] and Jing Xu [1,5*]

[1] State Key Laboratory of Chemical Engineering, School of Chemical Engineering, East China University of Science and Technology, Shanghai 200237, China

[2] Key Laboratory of Smart Manufacturing in Energy Chemical Process, Ministry of Education, East China University of Science and Technology, Shanghai 200237, China

[3] Key Laboratory for Green Chemical Technology of Ministry of Education Collaborative Innovation Center of Chemical Science and Engineering, School of Chemical Engineering and Technology, Tianjin University, Tianjin, 300072, China
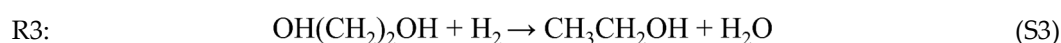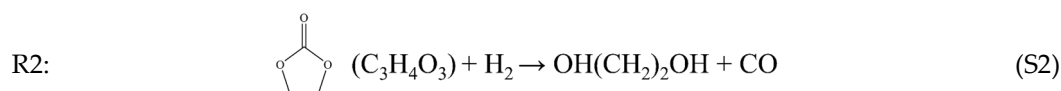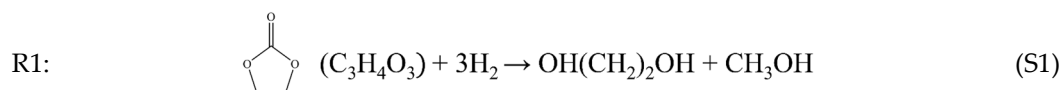
[4] Wison Engineering Ltd., 633 Zhongke Rd, Zhangjiang, Pudong, Shanghai, 201210, China

[5] Guangxi Key Laboratory of Petrochemical Resource Processing and Process Intensification Technology, School of Chemistry and Chemical Engineering, Guangxi University, Nanning 530004, China

Correspondence: caocx@ecust.edu.cn (Chenxi Cao); xujing@ecust.edu.cn (Jing Xu)

S1. Reaction kinetics

The reaction system of ethylene carbonate hydrogenation includes three reactions as follows:

R1: $(C_3H_4O_3) + 3H_2 \rightarrow OH(CH_2)_2OH + CH_3OH$ (S1)

R2: $(C_3H_4O_3) + H_2 \rightarrow OH(CH_2)_2OH + CO$ (S2)

R3: $OH(CH_2)_2OH + H_2 \rightarrow CH_3CH_2OH + H_2O$ (S3)
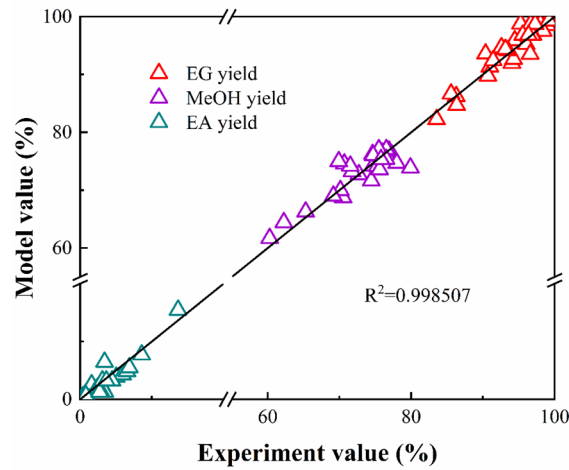
The intrinsic kinetic equations are as follows:

$$r_1 = A_1 \cdot e^{\frac{-Ea_1}{RT}} \cdot C_{EC}^{n_1} \cdot T^{n_1} \tag{S4}$$

$$r_2 = A_2 \cdot e^{\frac{-Ea_2}{RT}} \cdot C_{EC}^{n_2} \cdot T^{n_2} \tag{S5}$$

$$r_3 = A_3 \cdot e^{\frac{-Ea_3}{RT}} \cdot C_{EG}^{n_3} \cdot T^{n_3} \tag{S6}$$

Table S1. Intrinsic kinetic parameters.

	R1	R2	R3
A ([kmol, s])	1.01×10^1	2.11×10^0	2.54×10^8
Ea (kJ·mol^{-1})	30.1	28.1	113.8
n	0.65	1.00	0

Figure S1. Model and experiment values deviation of EC hydrogenation reaction.

In Figure S1, small deviation and high quality coefficient of determination ($R^2 = 0.998507$) mean that fitting of the model is good and reliable.

S2. Materials properties

S2.1. Physical properties

The density, heat capacity, thermal conductivity and viscosity of the gas mixture formula are as follows:

$$\rho_f = \frac{P_{op} \cdot M}{R \cdot T} \tag{S7}$$

$$c_{p,m} = \sum_i Y_i \, c_{p,i} \tag{S8}$$

$$k_f = \sum_i Y_i \, k_i \tag{S9}$$

$$\mu_m = \sum_i Y_i \, \mu_i \tag{S10}$$

Where Y_i is mass fraction of species i.

According to ASPEN database, the relations between properties parameters of each component ($c_{p,m}$, k_i, μ_i) and i, and the parameter values are shown in Table S2-S4.

Table S2. Specific heat capacity.

$c_{p,i} = A + BT + CT^2 + DT^3$ (323.15 K $< T <$ 523.15 K)			
A	**B**	**C**	**D**
EC [1]	4.032×10^2	2.096×10^0	/	/
EG [2]	4.810×10^2	2.583×10^0	/	/
MeOH [3]	6.147×10^2	2.501×10^0	/	/
C$_2$H$_5$OH	4.722×10^2	3.232×10^0	/	/
H$_2$O	1.986×10^3	-1.236×10^0	3.400×10^{-3}	-2.096×10^{-6}
H$_2$	1.151×10^4	1.695×10^1	-3.170×10^{-2}	1.983×10^{-5}
CO	1.089×10^3	-3.614×10^{-1}	7.247×10^{-4}	-2.108×10^{-7}

[1] EC is ethylene carbonate.
[2] EG is ethylene glycol.
[3] MeOH is methanol.

Table S3. Thermal conductivity.

$k_i = A + BT$ (323.15 K $< T <$ 523.15 K)		
	A	**B**
EC	-1.565×10^{-2}	8.367×10^{-5}
EG	-1.499×10^{-2}	8.839×10^{-5}
MeOH	-2.197×10^{-2}	1.202×10^{-4}
C$_2$H$_5$OH	-2.200×10^{-2}	1.202×10^{-4}
H$_2$O	-1.132×10^{-2}	9.569×10^{-5}
H$_2$	5.231×10^{-2}	4.278×10^{-4}
CO	6.200×10^{-3}	6.409×10^{-5}

Table S4. Viscosity.

$\mu_i = A + BT$ (323.15 K $< T <$ 523.15 K)		
	A	**B**
EC	-1.565×10^{-2}	8.367×10^{-5}
EG	-1.499×10^{-2}	8.839×10^{-5}
MeOH	-2.197×10^{-2}	1.202×10^{-4}
C$_2$H$_5$OH	-2.200×10^{-2}	1.202×10^{-4}
H$_2$O	-1.132×10^{-2}	9.569×10^{-5}
H$_2$	5.231×10^{-2}	4.278×10^{-4}
CO	6.200×10^{-3}	6.409×10^{-5}

S2.2.   EC condensation

EC partial pressure is compared with saturated vapor pressure to determine EC condensation. The saturated vapor pressure is obtained from the following formula:

$$\ln(P_{EC}^{sat}) = A + \frac{B}{T + C} + DT + E \ln T + FT^G \tag{S11}$$

where $A = 132.997$, $B = -13115$, $C = 0$, $D = 0$, $E = -17.579$, $F = 7.893 \times 10^{-6}$ and $G = 2$ from ASPEN database.
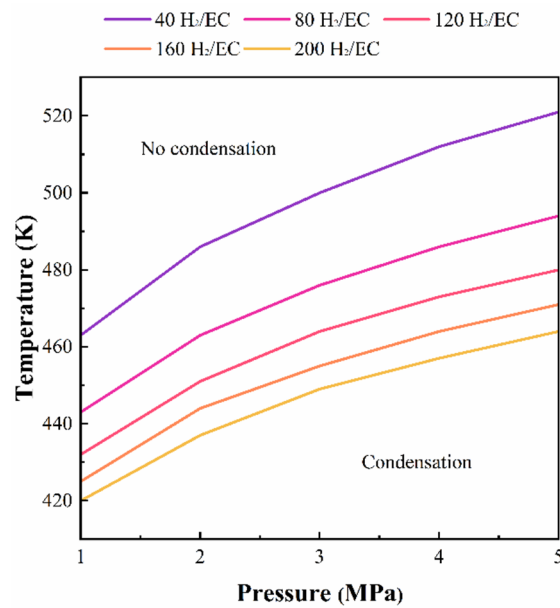
Figure S2. EC condensation zone under the condition of T = 410-530 K, P_{op} = 1-5 MPa and H$_2$/EC = 40-200.

EC condensation zone becomes larger as H₂/EC decreases from 200 to 40 in Figure S2.

S3. Transport properties

S3.1. Effective diffusion coefficient

The species mass transfer in the catalysts are related to effective diffusion coefficient $D_{\text{eff},i}$ that is computed by modified Bosanquet equation [1]:

$$D_{\text{eff},i} = \frac{\varepsilon_{\text{cat}}}{\tau}\left(\frac{1 - \alpha_{\text{M},i}X_i}{D_{\text{M},i}} + \frac{1}{D_{\text{k},i}}\right)^{-1} \tag{S12}$$

where molecular diffusion coefficient $D_{\text{M},i}$ and Kundsen diffusion coefficient $D_{\text{k},i}$ are calculated by Wilke equation [2]:

$$\frac{1}{D_{\text{M},i}} = \frac{1}{1 - X_i}\sum_{j \neq i}\frac{X_j}{D_{ij}} \tag{S13}$$

$$D_{\text{k},i} = \frac{d_{\text{pore}}}{3}\sqrt{\frac{8RT}{\pi M_i}} \tag{S14}$$

where binary diffusion coefficient D_{ij} is computed according to Chapman Enskog Kinetic theory [2]:

$$D_{ij} = 0.001858 \cdot T^{1.5}\frac{\left(\frac{1}{M_i} + \frac{1}{M_j}\right)^{0.5}}{P_{\text{op}}\sigma_{ij}^2\Omega_{\text{D}}} \tag{S15}$$

The species-average collision diameter σ_{ij} is computed by $\sigma_{ij} = (\sigma_i + \sigma_j)/2$ and the collision integral Ω_{D} is computed as follows:

$$\Omega_{\text{D}} = \frac{A}{T_{\text{N}}^B} + \frac{C}{\exp(DT_{\text{N}})} + \frac{E}{\exp(FT_{\text{N}})} + \frac{G}{\exp(HT_{\text{N}})} \tag{S16}$$

where $A = 1.0636$, $B = 0.1561$, $C = 0.193$, $D = 0.47635$, $E = 1.03587$, $F = 1.52996$, $G = 1.76474$, $H = 3.89411$ and $T_{\text{N}} = k_{\text{B}}T/\varepsilon_{ij}$.

S3.2. Oil heat transfer coefficient

Generally used equation Eq. S17 is to predict shell-side oil heat transfer coefficient, which is based on the weighted average mass velocity G_{l} [3].

$$\frac{\alpha_{\text{oil}}D_{\text{out}}}{k_{\text{oil}}} = 0.2\left(\frac{D_{\text{out}}G_{\text{l}}}{\mu}\right)^{0.6}\left(\frac{c_p\mu}{k_{\text{oil}}}\right)^{0.33}\left(\frac{\mu}{\mu_{\text{w}}}\right)^{0.14} \tag{S17}$$

$$G_{\text{l}} = \sqrt{G_{\text{b}}G_{\text{c}}} \tag{S18}$$

$$G_{\text{b}} = \frac{\dot{m}_{\text{oil}}}{3600 \cdot S_{\text{b}}} \tag{S19}$$

$$G_{\text{c}} = \frac{\dot{m}_{\text{oil}}}{3600 \cdot S_{\text{c}}} \tag{S20}$$

where G_b is mass velocity parallel with tubes and G_c is for cross-flow. And the baffle windows proportional of the shell cross section S_{b} and S_{c} are calculated by Eqs S25, S26 [3].

$$S_{\text{b}} = f_{\text{b}}\frac{\pi D_{\text{s}}^2}{4} - f_{\text{b}}N_{\text{t}}\frac{\pi D_{\text{out}}^2}{4} \tag{S21}$$

$$S_c = PD_s \left(1 - \frac{D_{out}}{p}\right) \tag{S22}$$

S4. Bed geometry

S4.1. Equivalent diameter

For cylinderical catalyst, equal specific surface area diameter (d_p^a), equal surface area diameter (d_p^s) and equal volume diameter (d_p^v) are defined as follows:

$$d_p^a = \left(0.5d + \frac{l}{d}\right)^{0.5} \tag{S23}$$

$$d_p^s = 3dl(d + 2l) \tag{S24}$$

$$d_p^v = d\left(\frac{3l}{2d}\right)^{\frac{1}{3}} \tag{S25}$$

S4.2. Bed voidage

Table S5. Bed voidage.

| Φ2 m adiabatic reactor		Φ0.05 m single tube $z = \frac{R-r}{d_p^v}$	
3 mm sphere	0.4	$z \leq 0.637$	$\varepsilon_b(r) = 2.14z - 2.53z + 1$
5 mm sphere	0.4		$\varepsilon_b(r) = 0.4 + 0.29\exp(-0.6z)$
7 mm sphere	0.4	$z > 0.637$	$\cdot \cos(2.3\pi z - 0.368\pi)$ $+0.15\exp(-0.9z)$
3×3 mm cylinder	0.304	$z < 0.84$ or $z > 1.04$	$\varepsilon_b(r) = 1 - 0.696 \cdot$ $\left[\begin{array}{c}1 - \exp(-1.819z^{0.342}) \cdot \\ \cos(6.64z^{1.077})\end{array}\right]$
5×5 mm cylinder	0.304		$\varepsilon_b(r) = 1 - 0.696 \cdot$
7×7 mm cylinder	0.304	$0.84 \leq z \leq 1.04$	$\left[\begin{array}{c}1 - \exp(-1.819z^{0.342}) \cdot \\ \cos(6.64z^{1.077})\end{array}\right]$ $+0.06\cos(5\pi(z - 0.54))$

## S5. Supplementary results

S5.1. Contours
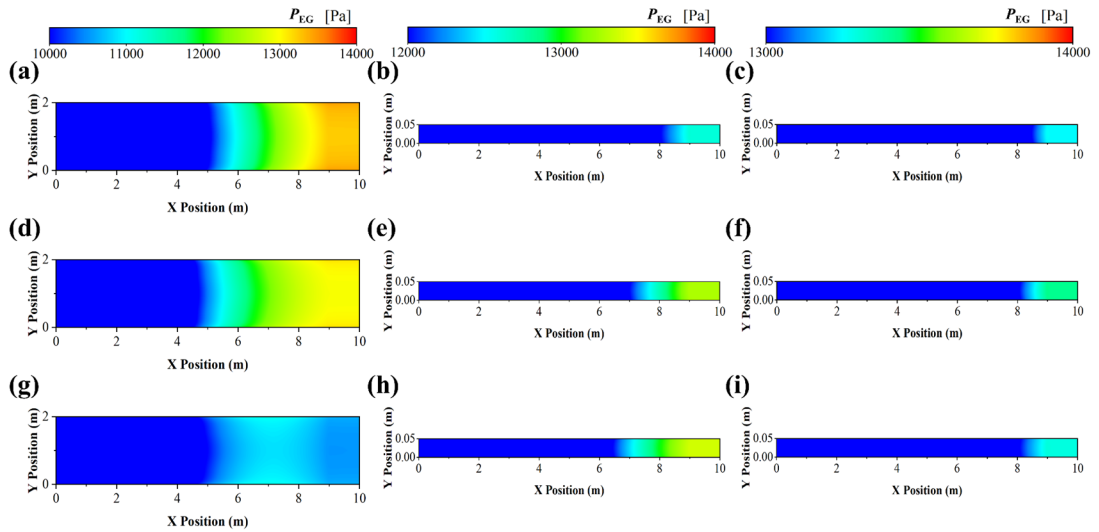
Figure S3. Contours of P_{EG} in different heat-exchange-type reactors: (a) (d) (g) adiabatic, (b) (e) (h) boiling water-cooled, (c) (f) (i) oil-cooled, under the conditions of 3 MPa, 0.3 $g_{EC}\cdot gcat^{-1}\cdot h^{-1}$, 200 H_2/EC

and inlet/coolant temperatures of (a) (d) (g) inlet temperatures 443, 463, 483 K, (b)/(c) (e)/(f) (h)/(i) inlet temperature 463 K, coolant temperatures 423, 443, 463 K.
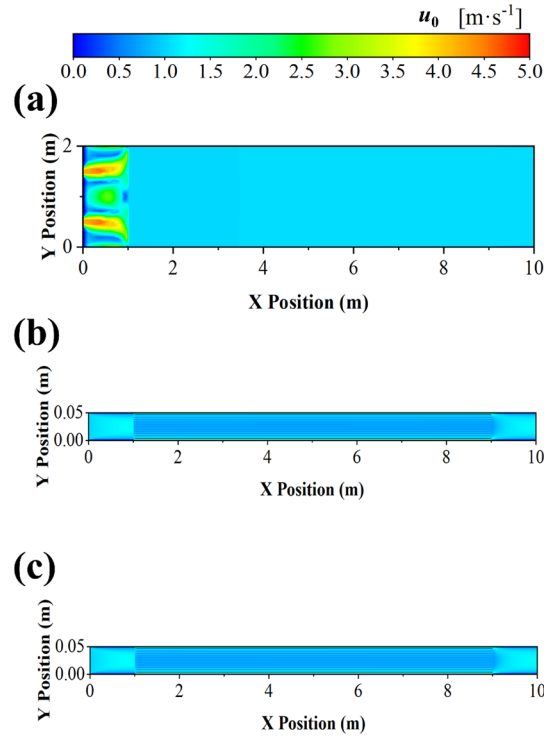

Figure S4. Contours of u_0 in different heat exchange type reactor: (a) adiabatic (b) boiling water-cooled (c) oil-cooled under the conditions of 3 MPa, 0.3 $g_{EC}·g_{cat}^{-1}·h^{-1}$, 200 H_2/EC, 463 K inlet temperature and 463 K coolant temperature.

*S5.2.   Velocity and bed pressure drop*
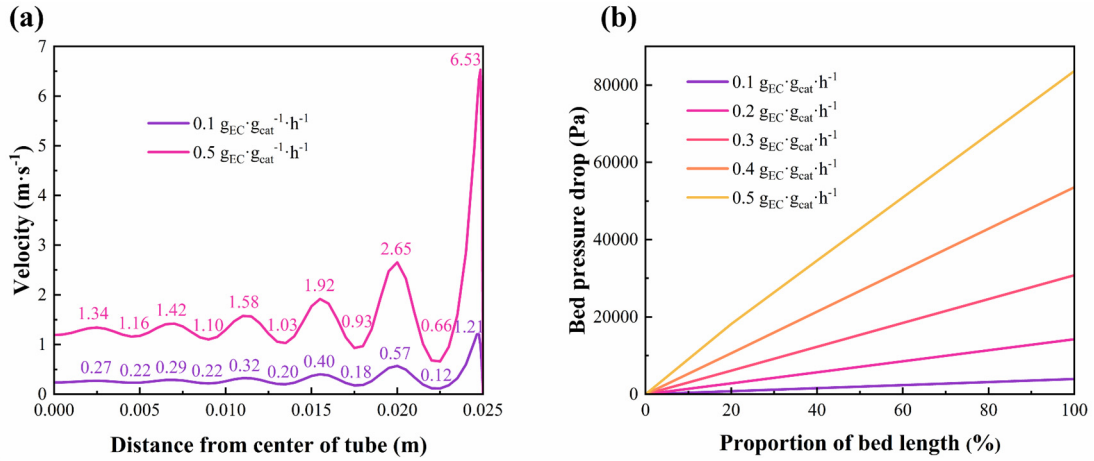
Figure S5. The influence of *SV* on (a) superficial velocity and (b) bed pressure drop, in boiling water-cooled reactor under the conditions of 3 MPa, 0.3 $g_{EC}·g_{cat}^{-1}·h^{-1}$ and 200 H_2/EC

S5.3.   Inlet/coolant temeprature
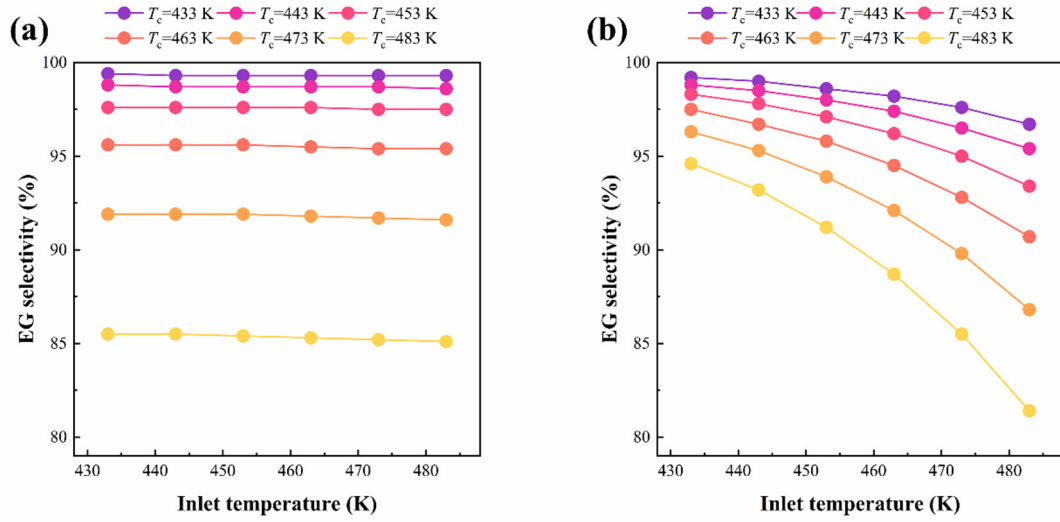
Figure S6. The influence of reactant/coolant inlet temperatures on S_{EG} under the conditions of 3 MPa, 0.3 $g_{EC} \cdot gcat^{-1} \cdot h^{-1}$ and 200 H_2/EC: (a) boiling water-cooled, (b) conduction oil-cooled reactor

In Figure S6, S_{EG} is determined by coolant inlet temperature not reactant inlet temperature in boiling water-cooled reactor. However, these two temperatures both affect S_{EG} in oil-cooled reactor.
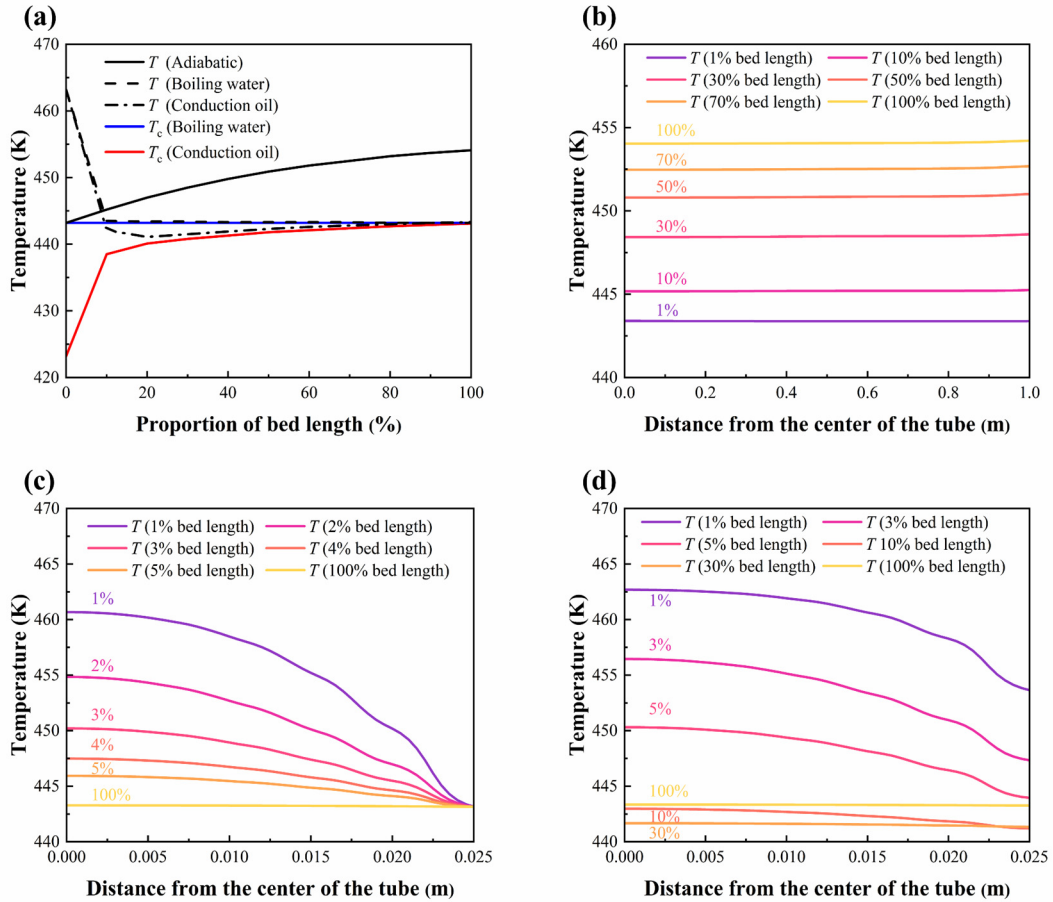
Figure S7. Under the conditions of 3 MPa, 0.3 $g_{EC} \cdot g_{cat}^{-1} \cdot h^{-1}$ and 200 H_2/EC, (a) bed and coolant temperatures in the axial direction; bed temperatures in the radial direction: (b) adiabatic, T_{in} = 443 K, (c) boiling water-cooled, T_{in} = 463 K and T_c = 443 K (d) conduction oil-cooled reactors, T_{in} = 463 K and T_c = 423 K

It can be seen from Figure S7a that the temperature rise of the adiabatic reactor bed is approximately 12 K. For boiling water-cooled, 463 K reactant temperature is cooled to 443 K as soon as it enters into the bed. The oil inlet temperature of oil-cooled reactor should be 423 K to cool the reactant to 443 K. According to the radial temperature distribution diagram of the bed (Figures S7b-d), the radial temperature of the adiabatic bed is very uniform, and the temperature of the bed with heat exchange is uneven in the front part. The temperature of boiling water-cooled bed is uniform after 5% length, and the radial temperature difference of oil-cooled bed is less than 2 K after 10% length. Different from boiling water-cooled, oil-cooled radial bed temperature first decreases and then increases. When the bed temperature is close to the oil temperature, the reaction heat release leads to temperature rise of oil (Figure S7a).

S5.4.   Catalyst size and shape

Table S6. Influence of catalyst sizes and shapes on reactor performance [1]

	3×3 mm cylinder	5×5 mm cylinder	7×7 mm cylinder	3 mm sphere	5 mm sphere	7 mm sphere
X_{EC} (%)	99.0	89.4	76.9	99.6	93.2	82.7
S_{EG} (%)	95.6	95.2	94.4	95.7	95.5	95.0
$S_{Alcohol}$ (%)	86.3	85.9	85.1	86.1	85.7	85.0
ΔP (kPa)	293	151	93	67	31	18
Yield of total alcohol (ton/a)	35209	31503	26709	29746	27158	23515

[1] Reactor type and conditions: Boiling water-cooled reactor, P_{op} = 3 MPa, SV = 0.3 $g_{EC} \cdot g_{cat} \cdot h^{-1}$, T_{in} = 463 K, T_c = 463 K and H_2/EC = 200.

Compare the same particle sizes and different shapes:
(1) For sphere catalyst, X_{EC} is higher and ΔP is lower.
(2) For cylinder catalyst, ε_b is lower, mass of filled catalysts is higher and yield of product is higher.
(3) S_{EG} and $S_{Alcohol}$ are nearly same for sphere and cylinder catalysts.
Compare the same shape and different particle sizes:
(1) For smaller catalyst, X_{EC} is higher and yield of product is higher.
(2) For larger catalyst, ΔP is lower.

S5.5.   Key variables effect

Table S7 Effect of key operating variables on X_{EC}, S_{EG}, S_{MeOH}

	T	H₂/EC	P_{op}	*SV*
Rise X_{EC}	High	High	High (Sensitive)	Low (Sensitive)
Rise S_{EG}	Low (Very Sensitive)	High for Adiabatic	/	High when SV < 0.2 $g_{EC} \cdot g_{cat}^{-1} \cdot h^{-1}$
Rise S_{MeOH}	High (Insensitive)	High (Insensitive)	Low (Insensitive)	Low (Insensitive)
No EC Condenses	High	High	Low	/

References

1. Plessis, J.P.; Diedericks, G. Fluid transport in porous media: Pore-scale modelling of interstitial transport phenomena. *Computational Mechanics Publications* **1997**, 61-104.
2. Bird, R.B.; Stewart, W.E.; Lightfoot, E.N. *Transport Phenomena*; John Wiley & Sons, Ltd: New York, United States, 1960.
3. McCabe, W.L.; Smith, J.C.; Harriott, P. Heat Tranfer to Fluids without Phase Change. In *Unit Operations in Chemical Engineering* Clark, B.J., E., C., Eds.; Mcgraw Hill, Inc.: New York, United States, 1993; pp. 330-373.